Quantitative Performance Analysis of Scalogram as Instantaneous Frequency Estimator

Ervin Sejdić, Igor Djurović, LJubiša Stanković

Abstract— **Instantaneous frequency (IF) estimation through the estimation of peak locations in the time-frequency plane is an important approach for signals contaminated with additive white Gaussian noise. In this paper, the forementioned analysis is carried out for continuous wavelet transform. The analysis of the scalogram as the instantaneous frequency estimator is performed for any FM signal regardless of the mother wavelet. Accurate expressions for the bias and the variance of the estimator are derived, and reveal that the bias and the variance are signal dependent. Results are statistically confirmed through the numerical analysis for several mother wavelets, and among considered wavelets, the Morlet wavelet produces the smallest estimation error. Furthermore, the performance of the IF estimator based on the scalogram and the spectrogram were compared through analysis of mean square error. These results showed that the scalogram with the Morlet wavelet exhibited good performance for the sample linear FM signal and the sample hyperbolic FM signal in comparison to the spectrogram.**

I. Introduction

Instantaneous frequency, usually defined as the derivative of the phase of a signal, is a fundamental concept present not only in communications (e.g. frequency modulation), but is also present in nature (e.g. changing color of light) [1], [2]. There are several approaches for the instantaneous frequency estimation, and extensive review of the topics is presented in [2], [3]. Some of these methods are parametric and some are nonparametric. In general, parametric methods use a signal model, and the goal is to estimate some parameters in order to obtain an estimate of the instantaneous frequency. Nonparametric methods on the other hand, do not require full knowledge of the signal and the time-frequency based approach is one of them. Originally, the basis for using the time-frequency distributions for the instantaneous frequency estimation is their first moment property [2], [4], [5]. However, the presence of noise leads to serious degradation of the first moment estimate [6]. As a consequence, the peak detection of time-frequency distribution is used instead and it is based on the detection of distribution peak positions.

Wavelet transform is a mathematical technique which decomposes a signal into both time and scale [7]. The transform uses specific analyzing functions, called wavelets, for the signal's decomposition, and the main property of these analyzing functions is that they are localized in time [8]. The scale decomposition is obtained by dilating or contracting the chosen analyzing wavelet before convolving it with the signal [9]. The parameter scale in the wavelet analysis is similar to the scale used in maps. As in the case of maps, high scales correspond to a non-detailed global view (of the signal), and low scales correspond to a detailed view. Similarly, in terms of frequency, low frequencies (high scales) correspond to global information of a signal (that usually spans the entire signal), whereas high frequencies (low scales) correspond to detailed information of the hidden pattern in a signal (that usually lasts a relatively short time). The limited time support of wavelets is important because then the behavior of the signal at infinity does not have a role. Therefore the wavelet analysis or synthesis can be performed locally on the signal, as opposed to the Fourier transform which is inherently nonlocal due to the space-filling nature of the trigonometric functions [10]. In addition, the wavelet transform has been applied

IEEE Transactions on Signal Processing, Vol. 56, No. 8, Aug. 2008.

in many different fields, such as biomedical applications [11], pattern recognition [12], power quality analysis [13], and computer graphics [14], to name a few.

The instantaneous frequency estimation based on the wavelet analysis was previously considered in several publications [15]-[20]. These works rely on the idea presented in [15], where an asymptotic approximation of the continuous wavelet transform using stationary phase approximation is considered. The authors showed that this asymptotic approximation can be used for the extraction of some characteristics of the analyzed signal, such as frequency and amplitude modulation laws. In order to estimate the instantaneous frequency of a signal, a so called ridge is used, which is essentially a peak in the time-frequency domain [16], [17]. For such an asymptotic approximation of the continuous wavelet transform, Cramer-Rao bounds for the instantaneous frequency variance at each time instant for the Morlet mother wavelet are investigated in [20]. The results depicted that in a specific case of the continuous wavelet transform with the Morlet mother wavelet, the transform achieved a performance close to the Cramer-Rao bounds especially at a low signal-to-noise ratio. The instantaneous frequency estimation from the phase of the continuous wavelet transform is also considered [18]. However, the results showed to be very unstable in practical situations when a signal is contaminated with noise. However, in all these works no attempts have been made to provide a general framework for the analysis of the scalogram as an instantaneous frequency estimator. Furthermore, the existing works usually only considered the behaviour of the Morlet wavelet.

The main contribution in this paper is a general analysis of the scalogram as the instantaneous frequency estimator for any FM signal. Expressions for bias and variance of such an estimator are derived regardless of the mother wavelet used in the analysis. These theoretical results are compared with the statistical data, i.e., the results of numerical analysis and high agreement between them is noticed. In addition, performances of the instantaneous frequency estimator based on the scalogram and spectrogram are compared through the magnitude of mean square errors. It is important to point out that the analysis of the scalogram based estimator is carried out based on determining the direct relationship between the scale and (Fourier) frequency for the mother wavelet. This is an important difference in comparison to the previous works, which assumed that the ridge actually corresponded to the IF of the signal, which is not necessarily the case.

This paper is organized as follows: In the next section a brief review of the wavelet transform is provided. Section III illustrates the performance of the instantaneous frequency estimator based on the wavelet transform, with in depth analysis of the bias and the variance of the estimation. In Section III-B bias and variance of the estimation error are derived for several commonly used mother wavelets. The obtained results are checked numerically and statistically in Section IV. Finally, conclusions are drawn in Section V.

II. Background Theory

A. Wavelet transform

The continuous wavelet transform (CWT) correlates the signal with families of waveforms that are well concentrated in time and frequency, and these families of waveforms are obtained by the dilations and translations of an analyzing wavelet, $\psi(t)$. Therefore, the CWT of a continuous signal $x(t)$ is defined as [7], [8], [10]:

$$CWT_c(t,s) = \int_{-\infty}^{+\infty} x(u)\frac{1}{\sqrt{s}}\psi^*\left(\frac{u-t}{s}\right)du \quad (1)$$

with $\psi(t)$ being the mother wavelet function, $\psi \in \mathbf{L^2}(\mathbb{R})$, where the mother wavelet satisfies the following condition

$$\int_{-\infty}^{+\infty} \psi(t)\,dt = 0. \quad (2)$$

If $u - t = \tau$ and

$$\Psi(t,s) = \frac{1}{\sqrt{s}}\psi\left(\frac{t}{s}\right) \quad (3)$$

are substituted in (1), then the CWT can be rewritten as:

$$CWT_c(t,s) = \int_{-\infty}^{+\infty} x(t+\tau)\Psi^*(\tau,s)d\tau. \quad (4)$$

In order to accurately relate the scale to the frequency, more precise relationships between the scale and the frequency were derived [21]-[23]. In particular, it has been shown that for a simple complex sinusoid, a relationship between the scale and the (Fourier) frequency can be found, so that the scale is a function of the frequency [21], [22], that is,

$$s = f(\omega) \quad (5)$$

and derivations for a general case are shown in Appendix A. Inherently, this relationship produces a time-frequency representation which is an unbiased estimator of the frequency for the simple sinusoids for non-noisy signals. Using the mentioned relationship the CWT can be rewritten as

$$CWT_c(t,\omega) = \int_{-\infty}^{+\infty} x(t+\tau)\Psi^*(\tau,\omega)d\tau. \quad (6)$$

The continuous wavelet transform of the discrete sequence $x(nT)$, sampled with a period T in τ, is defined as a convolution of the discrete sequence with a scaled and translated version of $\psi(nT)$:

$$CWT_d(t,\omega) = T\sum_n x(t+nT)\Psi^*(nT,\omega). \quad (7)$$

In the analysis using the short time Fourier transform, a spectrogram is defined as the square of amplitude of the time-frequency transformation of the signal, i.e., it is a time-frequency energy density function [4]. Similarly, in the wavelet analysis, the time-frequency energy density representation obtained by the wavelet transform is called scalogram, and it is defined as the square of amplitude of the wavelet transform:

$$W(t,\omega) = CWT_d(t,\omega)CWT_d^*(t,\omega) = \\ = T^2\sum_{n_1}\sum_{n_2}\{x(t+n_1T)x^*(t+n_2T)* \\ *\Psi^*(n_1T,\omega)\Psi(n_2T,\omega)\}. \quad (8)$$

B. Scalogram and IF estimation

Consider noisy discrete-time observations

$$x(nT) = f(nT) + \varepsilon(nT) \quad (9)$$

where $f(nT)$ is a sampled version of the continuous signal $f(t) = Ae^{j\phi(t)}$ with T being a sampling interval, and $\varepsilon(nT)$ is a complex-valued white Gaussian noise with i.i.d. real and imaginary parts. Thus, $\mathrm{Re}(\varepsilon(nT))$ and $\mathrm{Im}(\varepsilon(nT))$ are $\mathcal{N}(\prime, \sigma^{\in}/\in)$, and the total variance of the noise is equal to σ_ϵ^2. By definition, the instantaneous frequency of the considered signal is $\omega(t) = d\phi(t)/dt$. It should be assumed that $\omega(t)$ is an arbitrary smooth differentiable function of time with bounded derivatives $\left|\omega^{(r)}(t)\right| = \left|\phi^{(r)}(t)\right| \le M_r(t)$, $r \ge 1$.

The value of $\omega(t)$ can be estimated in the time-frequency plane as following [2], [6], [24]:

$$\hat{\omega}(t) = \arg\left[\max_{\omega\in Q_\omega} W(t,\omega)\right] \quad (10)$$

with $Q_\omega = \{\omega : 0 \le \omega \le \pi/T\}$ being a basic interval along the frequency axis. Before proceeding further, $W(t,\omega)$ for the signal $f(t)$ should be considered. Using the fact that the signal has a slow-varying amplitude and Taylor series expansion of the phase differences $f(t+n_1T)f^*(t+n_2T) = A^2e^{j\phi(t+n_1T)-j\phi(t+n_2T)}$, $W(t,\omega)$ can be expressed as

$$W(t,\omega) = \\ = T^2\sum_{n_1}\sum_{n_2}\Big\{A^2e^{j\Phi(n_1T,n_2T,t)+j\Delta\phi(n_1T,n_2T,t)}* \\ *\Psi^*(n_1T,\omega)\Psi(n_2T,\omega)\} \quad (11)$$

where $\Phi(n_1T,n_2T,t)$ represents the Taylor series approximation of the phase with first M terms, that is, $k = 0,\ldots,M$,

$$\Phi(n_1T,n_2T,t) \approx \sum_{k=0}^{M}\phi^{(k)}(t)\frac{(n_1T)^k-(n_2T)^k}{k!} \quad (12)$$

and

$$\Delta\phi(n_1T,n_2T,t) = \\ \sum_{k=M+1}^{\infty}\phi^{(k)}(t)\frac{(n_1T)^k-(n_2T)^k}{k!}, \quad (13)$$

where $\Delta\phi(n_1T, n_2T, t)$ represents a residue of the phase. Usually $\Delta\phi(n_1T, n_2T, t)$ represents the third and higher order terms. The estimation error, that is, the difference between $\omega(t)$ and estimated peak frequencies, at a time-instant, t, is defined as

$$\triangle\hat{\omega}(t) = \omega(t) - \hat{\omega}(t) \tag{14}$$

and due to the presence of the white Gaussian noise, the estimation error, $\triangle\hat{\omega}(t)$, can be considered to be a random variable as well, characterized by its bias and variance.

III. Performance Analysis of the IF estimator

The estimate of the IF, $\hat{\omega}(t)$, is defined by the stationary point of $W(t,\omega)$ [25]. It can be found by setting the derivative $\partial W(t,\omega)/\partial\omega$ to zero, that is, $\partial W(t,\omega)/\partial\omega = 0$, where

$$\frac{\partial W(t,\omega)}{\partial\omega} =$$

$$= T^2 \sum_{n_1}\sum_{n_2} \{x(t+n_1T)x^*(t+n_2T)*$$

$$* \left[\frac{\partial\Psi^*(n_1T,\omega)}{\partial\omega}\Psi(n_2T,\omega)+\right.$$

$$\left.+\Psi^*(n_1T,\omega)\frac{\partial\Psi(n_2T,\omega)}{\partial\omega}\right]\Big\}. \tag{15}$$

In order to perform the estimation error analysis, we linearize $\partial W(t,\omega)/\partial\omega$ around the stationary point with respect to small estimation error $\triangle\hat{\omega}(t)$, phase residue $\triangle\phi$ and noise ε [25]-[32]:

$$\frac{\partial W(t,\omega)}{\partial\omega}|_0 + \frac{\partial^2 W(t,\omega)}{\partial\omega^2}|_0 \triangle\hat{\omega}(t)+$$

$$+\frac{\partial W(t,\omega)}{\partial\omega}|_{0\delta_{\triangle\phi}} + \frac{\partial W(t,\omega)}{\partial\omega}|_{0\delta_\varepsilon} = 0 \tag{16}$$

where $|_0$ indicates that the derivatives are calculated at the point $\omega = \phi^{(1)}(t)$, $\triangle\phi = 0$, and $\varepsilon = 0$. The terms $\partial W(t,\omega)/\partial\omega|_{0\delta_{\triangle\phi}}$ and $\partial W(t,\omega)/\partial\omega|_{0\delta_\varepsilon}$ represent variations of the derivative $\partial W(t,\omega)/\partial\omega$ caused by small $\Delta\phi(n_1T, n_2T, t)$ and noise $\varepsilon(nT)$, respectively [27].

The terms from (16) are defined as [26]:

$$\frac{\partial W(t,\omega)}{\partial\omega}|_0 = 2T^2A^2\,\mathrm{Re}\{P(t,\omega)E(t,\omega)\} \tag{17}$$

$$\frac{\partial^2 W(t,\omega)}{\partial\omega^2}|_0 =$$

$$= -2T^2A^2\left[R(t,\omega)E(t,\omega) - |P(t,\omega)|^2\right] \tag{18}$$

$$\frac{\partial W(t,\omega)}{\partial\omega}|_{0\delta_{\triangle\phi}} = 2T^2A^2\,\mathrm{Re}\{Q(t)F(t)\} \tag{19}$$

whereas $\partial W(t,\omega)/\partial\omega|_{0\delta_\varepsilon}$ will be given separately. The functions $E(t,\omega)$, $F(t,\omega)$, $P(t,\omega)$, $Q(t,\omega)$, and $R(t,\omega)$ are also calculated at the point $\omega = \phi^{(1)}(t)$ and are defined by

$$E(t,\omega) = \sum_n e^{-j\omega nT}\Psi(nT,\omega) \tag{20}$$

$$F(t,\omega) = \sum_n e^{-j\omega nT - j\Delta\phi(nT,t)}\Psi(nT,\omega) \tag{21}$$

$$P(t,\omega) = \sum_n e^{j\omega nT + j\phi^{(2)}(t)\frac{(nT)^2}{2}}\frac{\partial\Psi^*(nT,\omega)}{\partial\omega} \tag{22}$$

$$Q(t,\omega) = \sum_n \left\{e^{j\omega nT + j\phi^{(2)}(t)\frac{(nT)^2}{2} + j\Delta\phi(nT,t)}\right.$$

$$\left.\times\frac{\partial\Psi^*(nT,\omega)}{\partial\omega}\right\} \tag{23}$$

$$R(t,\omega) = \sum_n e^{j\omega nT}\frac{\partial^2\Psi^*(nT,\omega)}{\partial\omega^2} \tag{24}$$

where for $M = 2$, the approximation

$$e^{j\sum_{k=0}^{2}\phi^{(k)}(t)\frac{(nT)^k}{k!}} \cong$$

$$\cong e^{j\left(\phi(t)+\phi^{(1)}(t)(nT)\right)}\left(1 + j\phi^{(2)}(t)\frac{(nT)^2}{2}\right) \tag{25}$$

is used to simplify the above expression.

A. IF Estimation Bias and Variance

Using the derived equations (17)-(19), the equation (16) is rewritten in a general form as (eq. 26)

Theorem III.1: Let $\hat{\omega}(t)$ be a solution of (10) and $T \to 0$, then the bias of the IF estimation error $\triangle\hat{\omega}(t)$ is given by eq. 27

$$\triangle\hat{\omega}(t) = \frac{2T^2A^2\,\mathrm{Re}\left\{P(t,\omega)E(t,\omega)\right\} + 2T^2A^2\,\mathrm{Re}\left\{Q(t,\omega)F(t,\omega)\right\} + \frac{\partial W(t,\omega)}{\partial\omega}|_{0\delta_\varepsilon}}{2T^2A^2\left[R(t,\omega)E(t,\omega) - |P(t,\omega)|^2\right]}. \tag{26}$$

$$\mathrm{bias}\left(\triangle\hat{\omega}(t)\right) = \frac{4T^2A^2\,\mathrm{Re}\left\{P(t,\omega)E(t,\omega)\right\} + 2T^2A^2\,\mathrm{Re}\left\{Q(t,\omega)F(t,\omega)\right\} + \sigma^2T^2\left(B_1+B_2\right)}{2T^2A^2\left[R(t,\omega)E(t,\omega) - |P(t,\omega)|^2\right]} \tag{27}$$

where

$$B_1 = \sum_n \frac{\partial\Psi^*(nT,\omega)}{\partial\omega}\Psi(nT,\omega) \tag{28}$$

$$B_2 = \sum_n \Psi^*(nT,\omega)\frac{\partial\Psi(nT,\omega)}{\partial\omega}. \tag{29}$$

Proof: The general expression of the estimation error is given by (26), and the only random term is $\partial W(t,\omega)/\partial\omega|_{0\delta_\varepsilon}$. Therefore, the expected value of the estimation error, that is, the bias is given by eq. 30

The expected value of $\partial W(t,\omega)/\partial\omega|_{0\delta_\varepsilon}$ is given by eq. 31which results in

The above equation is equal to (27), which proves the second part of the theorem. □

Special Case: A linear FM signal $f(t) = Ae^{j\frac{a}{2}t^2}$ corrupted by a stationary, complex, additive, white Gaussian noise yields the IF bias:

$$\mathrm{bias}\left(\triangle\hat{\omega}(t)\right) = $$

$$= \frac{6A^2\,\mathrm{Re}\left\{P(t,\omega)E(t,\omega)\right\} + \sigma^2\left(B_1+B_2\right)}{2A^2\left[R(t,\omega)E(t,\omega) - |P(t,\omega)|^2\right]} \tag{33}$$

since $\Delta\phi(n_1T,n_2T,t) = 0$ resulting in variations of the derivative $\partial W(t,\omega)/\partial\omega$ caused by small $\Delta\phi(n_1T,n_2T,t)$ being equal to (17).

***Theorem** III.2:* Let $\hat{\omega}(t)$ be a solution of (10) and $T \to 0$, then the variance of the IF estimation error $\triangle\hat{\omega}(t)$ is given by where

$$B_3 = \sum_n \frac{\partial\Psi^*(nT,\omega)}{\partial\omega}\frac{\partial\Psi(nT,\omega)}{\partial\omega} \tag{35}$$

$$B_4 = \sum_n \Psi(nT,\omega)\Psi^*(nT,\omega) \tag{36}$$

$$\Omega(t,\omega) = $$

$$= T^4\sigma^2\left(4B_1+2B_2\right)P(t,\omega)E(t,\omega) +$$

$$+T^4\sigma^2\left(2B_1+4B_2\right)E^*(t)P^*(t)$$

$$+2T^4\sigma^2B_4\left|P(t,\omega)\right|^2 + 2T^4\sigma^2B_3\left|E(t,\omega)\right|^2$$

$$-4\sigma^2T^4A^2\,\mathrm{Re}\left\{P(t,\omega)E(t,\omega)\right\}\left(B_1+B_2\right). \tag{37}$$

Proof: By definition, the variance is given by

$$\mathrm{var}\left(\triangle\hat{\omega}(t)\right) = E\left\{\left(\triangle\hat{\omega}(t)\right)^2\right\} - E\left\{\triangle\hat{\omega}(t)\right\}^2 \tag{38}$$

where the first term is equal to eq. 39, and the second term is equal to eq. 40. By simple algebraic manipulation of the above equations, the variance can be written as eq 41. It can be shown that eq 42. By substituting the above equation in the previous equation, we will obtain the expression for variance given by (34). □

B. IF Estimation With Specific Wavelets

The expressions for the bias and the variance in the case of any wavelet may be obtained as special cases of (27) and (34). Let us write these expressions for several important mother wavelets given by:

- a Mexican hat [7]:

$$\psi(t) = \frac{2}{\pi^{1/4}\sqrt{3\zeta}}\left(\frac{t^2}{\zeta^2} - 1\right)\exp\left(-\frac{t^2}{2\zeta^2}\right) \tag{43}$$

where $\zeta = 1$;

- a modified Morlet wavelet [10]:

$$\psi(t) = \frac{1}{\sqrt{2\pi}}\exp(j\eta t - t^2/2) \tag{44}$$

where $\eta = \pi\sqrt{2/\ln(2)}$;

- a Cauchy wavelet [9]:

$$\psi(t) = \frac{1}{2\pi}\frac{1}{(1-jt)^2}. \tag{45}$$

Using the procedure outlined in Appendix A, the scale to frequency relations for the three

$$E\left\{\triangle\hat{\omega}(t)\right\}=\frac{2T^2A^2\,\mathrm{Re}\left\{P(t,\omega)E(t,\omega)\right\}+2T^2A^2\,\mathrm{Re}\left\{Q(t,\omega)F(t,\omega)\right\}+E\left\{\frac{\partial W(t,\omega)}{\partial\omega}|_{0\delta_\varepsilon}\right\}}{2T^2A^2\left[R(t,\omega)E(t,\omega)-|P(t,\omega)|^2\right]}. \tag{30}$$

$$\begin{aligned}E\left\{\frac{\partial W(t,\omega)}{\partial\omega}|_{0\delta_\varepsilon}\right\}&=E\left\{T^2\sum_{n_1}\sum_{n_2}x(n_1T+t)x^*(n_2T+t)\frac{\partial\Psi^*(n_1T,\omega)}{\partial\omega}\Psi(n_2T,\omega)\right\}\\&+E\left\{T^2\sum_{n_1}\sum_{n_2}x(n_1T+t)x^*(n_2T+t)\Psi^*(n_1T,\omega)\frac{\partial\Psi(n_2T,\omega)}{\partial\omega}\right\}\\&=T^2\sum_{n_1}\sum_{n_2}A^2e^{j\Phi(n_1T,n_2T,t)}\\&\times\left[\frac{\partial\Psi^*(n_1T,\omega)}{\partial\omega}\Psi(n_2T,\omega)+\Psi^*(n_1T,\omega)\frac{\partial\Psi(n_2T,\omega)}{\partial\omega}\right]\\&+T^2\sigma^2\sum_n\left[\frac{\partial\Psi^*(nT,\omega)}{\partial\omega}\Psi(nT,\omega)+\Psi^*(nT,\omega)\frac{\partial\Psi(nT,\omega)}{\partial\omega}\right]\\&=\frac{\partial W(t,\omega)}{\partial\omega}|_0+\sigma^2T^2\left(B_1+B_2\right)\end{aligned} \tag{31}$$

$$E\left\{\triangle\hat{\omega}(t)\right\}=\frac{4T^2A^2\,\mathrm{Re}\left\{P(t,\omega)E(t,\omega)\right\}+2T^2A^2\,\mathrm{Re}\left\{Q(t,\omega)F(t,\omega)\right\}+\sigma^2T^2\left(B_1+B_2\right)}{2T^2A^2\left[R(t,\omega)E(t,\omega)-|P(t,\omega)|^2\right]}. \tag{32}$$

TABLE I
SCALE TO FREQUENCY RELATIONSHIPS FOR THE CONSIDERED WAVELETS.

Wavelet	**Relation**
Mexican hat	$s=\frac{\sqrt{10}}{2\zeta\omega}$
Morlet	$s=\frac{\eta+\sqrt{\eta^2+2}}{2\omega}$
Cauchy	$s=\frac{3}{2\omega}$

considered wavelets are summarized in Table I.

Before proceeding further on, it is worthwhile to closely examine terms B_1 and B_2. As $T\to 0$, we have

$$TB_1\to\int_{-\infty}^{+\infty}\frac{\partial\Psi^*(\tau,\omega)}{\partial\omega}\Psi(\tau,\omega)d\tau \tag{46}$$

$$TB_2\to\int_{-\infty}^{+\infty}\Psi^*(\tau,\omega)\frac{\partial\Psi(\tau,\omega)}{\partial\omega}d\tau \tag{47}$$

and for the three considered wavelets, it can be shown that

$$B_1=B_2=0. \tag{48}$$

Since the considered wavelets are Hermitian functions, it is also straightforward to show that B_1 is a complex conjugate of B_2, that is, $B_1=B_2^*$. Hence, for any wavelets that are Hermitian functions, it is sufficient to find one of the values.

$$\mathrm{var}\left(\triangle\hat{\omega}(t)\right)=\frac{\Omega(t,\omega)+T^4\sigma^4B_1^2+4T^4\sigma^4B_1B_2+2T^4\sigma^4B_3B_4+T^4\sigma^4B_2^2}{4T^4A^4\left[R(t,\omega)E(t,\omega)-|P(t,\omega)|^2\right]^2} \tag{34}$$

Therefore, the bias and variance of estimation error are equal to

$$\text{bias}\left(\triangle\hat{\omega}(t)\right) = \frac{2\,\text{Re}\left\{P(t,\omega)E(t,\omega)\right\} + \text{Re}\left\{Q(t,\omega)F(t,\omega)\right\}}{\left[R(t,\omega)E(t,\omega) - |P(t,\omega)|^2\right]} \tag{49}$$

$$\text{var}\left(\triangle\hat{\omega}(t)\right) = \frac{\sigma^2 B_4 |P(t,\omega)|^2 + \sigma^2 B_3 |E(t,\omega)|^2 + \sigma^4 B_3 B_4}{2A^4\left[R(t,\omega)E(t,\omega) - |P(t,\omega)|^2\right]^2}. \tag{50}$$

Similarly, as for B_1 and B_2, we can find values for B_3 and B_4 as $T \to 0$ and these are summarized in Table II. It is clear that $B_3 \sim 1/T\omega^2$, while $B_4 \sim 1/T$ for the three considered wavelets.

$$E\left\{\left(\triangle\hat{\omega}(t)\right)^2\right\} = \left[\left(\frac{\partial W(t,\omega)}{\partial\omega}|_0\right)^2 + \left(\frac{\partial W(t,\omega)}{\partial\omega}|_{0\delta_{\triangle\phi}}\right)^2 + E\left\{\left(\frac{\partial W(t,\omega)}{\partial\omega}|_{0\delta_\varepsilon}\right)^2\right\} + 2\frac{\partial W(t,\omega)}{\partial\omega}|_0\frac{\partial W(t,\omega)}{\partial\omega}|_{0\delta_{\triangle\phi}} + 2\frac{\partial W(t,\omega)}{\partial\omega}|_0 E\left\{\frac{\partial W(t,\omega)}{\partial\omega}|_{0\delta_\varepsilon}\right\} + 2\frac{\partial W(t,\omega)}{\partial\omega}|_{0\delta_{\triangle\phi}} E\left\{\frac{\partial W(t,\omega)}{\partial\omega}|_{0\delta_\varepsilon}\right\}\right] \Bigg/ \left(\frac{\partial^2 W(t,\omega)}{\partial\omega^2}|_0\right)^2 \tag{39}$$

$$E\left\{\triangle\hat{\omega}(t)\right\}^2 = \left[\left(\frac{\partial W(t,\omega)}{\partial\omega}|_0\right)^2 + \left(\frac{\partial W(t,\omega)}{\partial\omega}|_{0\delta_{\triangle\phi}}\right)^2 + E\left\{\frac{\partial W(t,\omega)}{\partial\omega}|_{0\delta_\varepsilon}\right\}^2 + 2\frac{\partial W(t,\omega)}{\partial\omega}|_0\frac{\partial W(t,\omega)}{\partial\omega}|_{0\delta_{\triangle\phi}} + 2\frac{\partial W(t,\omega)}{\partial\omega}|_0 E\left\{\frac{\partial W(t,\omega)}{\partial\omega}|_{0\delta_\varepsilon}\right\} + 2\frac{\partial W(t,\omega)}{\partial\omega}|_{0\delta_{\triangle\phi}} E\left\{\frac{\partial W(t,\omega)}{\partial\omega}|_{0\delta_\varepsilon}\right\}\right] \Bigg/ \left(\frac{\partial^2 W(t,\omega)}{\partial\omega^2}|_0\right)^2. \tag{40}$$

$$\begin{aligned}\text{var}\left(\triangle\hat{\omega}(t)\right) &= \frac{E\left\{\left(\frac{\partial W(t,\omega)}{\partial\omega}|_{0\delta_\varepsilon}\right)^2\right\} - E\left\{\frac{\partial W(t,\omega)}{\partial\omega}|_{0\delta_\varepsilon}\right\}^2}{\left(\frac{\partial^2 W(t,\omega)}{\partial\omega^2}|_0\right)^2} \\ &= \frac{E\left\{\left(\frac{\partial W(t,\omega)}{\partial\omega}|_{0\delta_\varepsilon}\right)^2\right\} - \left(\frac{\partial W(t,\omega)}{\partial\omega}|_0 + \sigma^2 T^2\left(B_1 + B_2\right)\right)^2}{\left(\frac{\partial^2 W(t,\omega)}{\partial\omega^2}|_0\right)^2}.\end{aligned} \tag{41}$$

$$\begin{aligned}E\left\{\left(\frac{\partial W(t,\omega)}{\partial\omega}|_{0\delta_\varepsilon}\right)^2\right\} &= \left(\frac{\partial W(t,\omega)}{\partial\omega}|_0\right)^2 + T^4\sigma^2\left(4B_1 + 2B_2\right)P(t,\omega)E(t,\omega) \\ &\quad + T^4\sigma^2\left(2B_1 + 4B_2\right)E^*(t,\omega)P^*(t,\omega) + 2T^4\sigma^2 B_4|P(t,\omega)|^2 + 2T^4\sigma^4 B_1^2 \\ &\quad + 2T^4\sigma^2 B_3|E(t,\omega)|^2 + 2T^4\sigma^4 B_1 B_2 + 2T^4\sigma^4 B_3 B_4 + 2T^4\sigma^4 B_2^2.\end{aligned} \tag{42}$$

TABLE II
VALUES OF B_3 AND B_4 FOR THE CONSIDERED WAVELETS.

	Mexican hat	**Morlet**	**Cauchy**
B_3	$\frac{5}{2\omega^2 T}$	$\frac{\eta^2+1}{4\omega^2 T\sqrt{\pi}}$	$\frac{3}{32\pi T\omega^2}$
B_4	$\frac{1}{T}$	$\frac{1}{2T\sqrt{\pi}}$	$\frac{1}{8\pi T}$

IV. Numerical Analysis

In this section the performance of the scalogram based IF estimator is checked numerically. The goal of the numerical analysis is to examine whether the theoretical expressions derived in the previous section correspond to the actual results of simulations. Also, the mean square error (MSE) of the IF estimation for the scalogram using the considered wavelets will be compared to the MSE obtained by the spectrogram [26], [28]. The purpose of this part of the study is to examine how the results obtained by the scalogram compare to the results obtained by other classical method.

A. Comparison among different wavelets

In this section, the performance of the IF estimator is examined using two classes of signals. A linear FM signal $f_1(t) = \exp\left(j128\pi t + j\frac{\alpha}{2}t^2\right)$ is considered for $0 < \alpha \leq 16\pi$ and a hyperbolic FM signal $f_2(t) = \exp\left(j\beta \text{sign}(t)\ln(|t|+1)\right)$ is considered for $0 < \beta \leq 256\pi$. The sampling period used is $T = 1/256$ with 512 data points, and the variance of the noise used in the analysis is set to $\sigma_\epsilon^2 = 0.1$. The results of the numerical analysis along with the theoretical values are depicted in Figs. 1 and 2, and they represent the bias and the variance for the lag at $t = 0.5$, that is, $W(0.5, \omega)$.

Theoretical values are produced by applying the derived expressions (27) and (34) for the particular signals, while the statistical data are obtained by 10000 realizations. The vertical axis represents the magnitude of the estimation bias and variance, while the horizontal axis represents the values of variables (α and β).

A very high agreement between the theoretical and statistical results for the linear FM signal can easily be observed in Fig. 1 for all cases except for the bias obtained by the scalogram with the Morlet wavelet. The reason for disagreement in the case of this particular wavelet is the amplitude of the bias. The biggest bias is obtained for $\alpha = 16\pi$ and is of order of 10^{-4}, which is 1000 times smaller than the variance of the noise used in the numerical analysis.

For the hyperbolic class of signals, the theoretical values of the bias and the variance also have high agreement with the results of the numerical analysis. While for all mother wavelets the values of the bias and the variance are increasing for the linear FM signal, here it can be noticed that the Morlet wavelet produces decreasing values of the bias.

We have examined how the estimation bias and variance behave for two classes of signals and several wavelets. In order to further gain understanding of the differences among wavelets, the MSE of the estimation is examined as well for the given scenarios. The MSE is obtained as a sum of the variance and squared bias, and the results are depicted in Figs. 3(a) and (b).

From these figures, it is clear that the Morlet wavelet produces significantly lower MSE in comparison to other wavelets for both classes of signals. For the linear FM signals and hyperbolic class of signals, the Cauchy wavelet produces the biggest error.

B. Comparison of Scalogram with Spectrogram

In this section, the MSE of the IF estimator obtained by the scalogram, $W(t, \omega)$, and a spectrogram is examined using two signals. A linear FM signal $f_3(t) = \exp\left(j60\pi t + j\frac{\alpha}{2}t^2\right)$ is considered for $\alpha = 30\pi$ and a hyperbolic FM signal $f_4(t) = \exp\left(j\beta \text{sign}(t)\ln(|t|+1)\right)$ is considered for $\beta = 64\pi$. The sampling period used is $T = 1/256$ with 512 data points. The signals are contaminated with a white Gaussian noise, and the signal to noise ratio (SNR) is given by $SNR = 10\log_{10}(A^2/\sigma^2)$ with $A = 1$ being a signal's amplitude and σ^2 being the variance of the noise. The SNR is varied from 0 dB to 15 dB by a 1-dB step. For each SNR value, 1000 realizations are used. The estimation is performed using position of maxima of

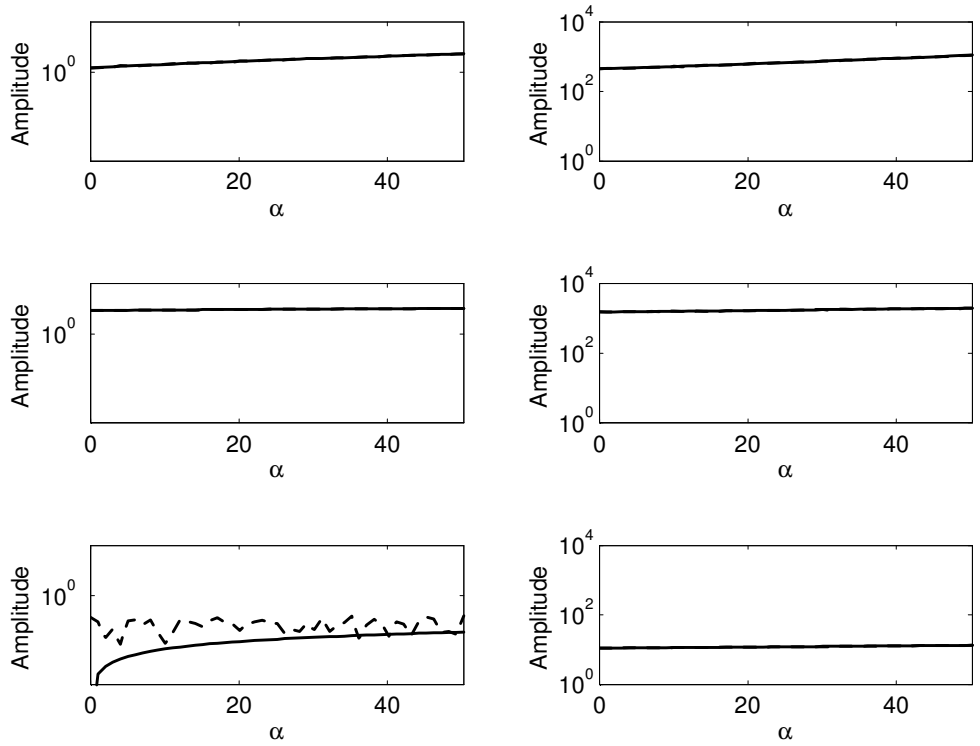

Fig. 1. IF bias and variance obtained theoretically (solid) and statistically (dashed) as a function of α: (a) bias and variance for the Mexican hat wavelet; (b) bias and variance for the Cauchy wavelet; (c) bias and variance for the Morlet wavelet.

the scalograms and spectrogram [28]. In calculation of the spectrogram, a Gaussian window is used for several values of σ given by $\sigma = \{0.005, 0.01, 0.015\}$.

Figs. 4 and 5 represent the results of such an analysis. The horizontal axis represents the SNR (in decibels), and the vertical axis represents the MSE for the instantaneous frequency estimation. For the linear FM signal, the results depict an expected situation. The spectrogram generally provides lower MSE in comparison to the scalogram due to the fact that with a proper choice of a window function it can provide a more concentrated time-frequency representation than the scalogram. It is worthwhile noting that the scalogram with the Morlet mother wavelet also provides good performance in comparison to the spectrogram for the chosen linear FM signal.

For the hyperbolic signal, the best performance is exhibited by the scalogram with the Morlet mother wavelet. This performance is expected, since the scalograms are usually capable of achieving higher concentration of hyperbolic signals in the time-frequency domain than the spectrograms due to their variable resolution property.

Even though the presented numerical analysis provided hints about the performance of both the spectrogram and the scalogram, further generalizations should be avoided unless a rigorous comparative analysis is completed. As stated previously, Figs. 4 and 5 depict expected results for the sample signals. These results are expected based on the properties of the implemented time-frequency representations, i.e., an ability to provide good localization of energy concentration for specific classes of signals.

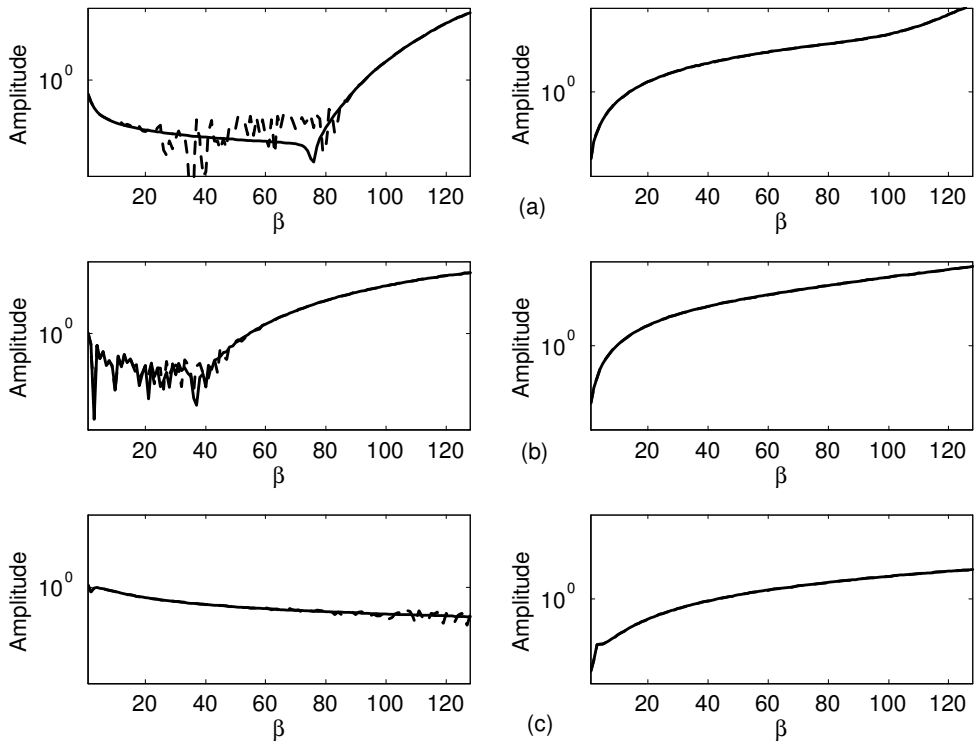

Fig. 2. IF bias and variance obtained theoretically (solid) and statistically (dashed) as a function of β: (a) bias and variance for the Mexican hat wavelet; (b) bias and variance for the Cauchy wavelet; (c) bias and variance for the Morlet wavelet.

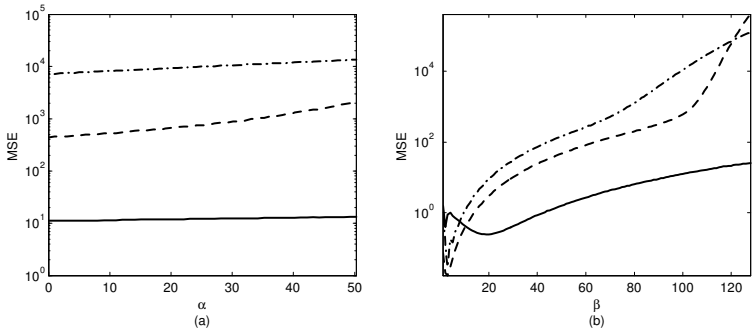

Fig. 3. MSE of the IF estimation (variance plus squared bias) for the Mexican hat wavelet (dashed), the Cauchy wavelet (dashdot) and the Morlet wavelet (solid lane) as a function of: (a) α; (b) β.

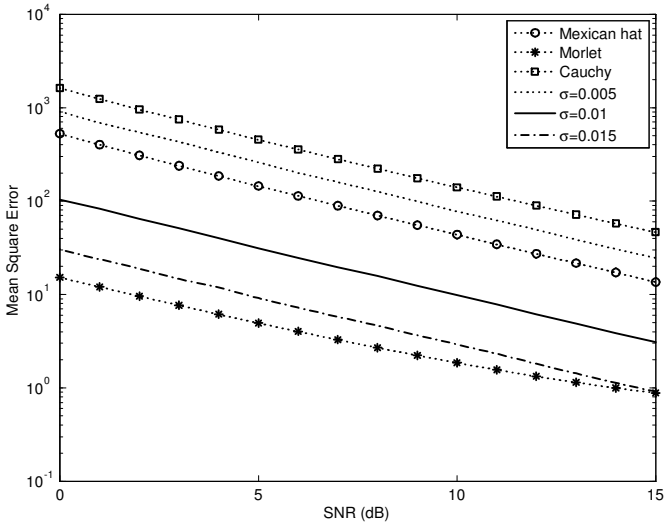

Fig. 4. Comparison of the MSE for linear FM signal for several different mother wavelets and STFT with three different window widths.

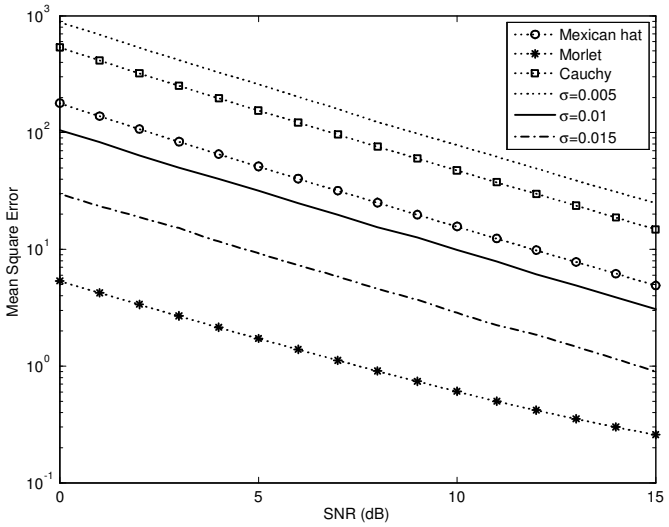

Fig. 5. Comparison of the MSE for several different mother wavelets and STFT with several different window widths.

V. Conclusion

In this paper, a general analysis of the scalogram as the instantaneous frequency estimator for FM signals contaminated with the additive white Gaussian noise was performed. Expression for the bias and the variance of such an estimator were derived regardless of the mother wavelet used in the analysis. The analysis of the estimator was performed without using the asymptotic approximation of the continuous wavelet transform and is based on determining the direct relationship between the scale and (Fourier) frequency for the mother wavelet. Several mother wavelets were considered including Morlet wavelet, Cauchy wavelet and Mexican hat wavelet. The theoretical results were compared with the results of numerical analysis and high agreement between

them was noticed. By comparing the results of the analysis, it was noticed that the scalogram with the Morlet wavelet exhibited the best performance for linear FM signals and hyperbolic FM signals. In addition, the performance of the instantaneous frequency estimator based on the scalogram and the spectrogram were compared through the magnitude of MSE. These results also depicted that the scalogram with the Morlet wavelet exhibited good performance for the sample linear FM signal and the sample hyperbolic FM signal in comparison to the spectrogram.

Appendix A

In order to understand how to find the relationship given by (5), consider the signal $x(t) = A\exp(j\omega_o t)$. Then the CWT of the signal for the wavelet $\psi(t)$ is given by (1). In order to find an analytical expression of the CWT, we express the CWT in terms of the Fourier transforms of the signal, $X(\omega)$, and mother wavelet, $\Phi(\omega)$, as

$$CWT_x(t,s) =$$

$$\frac{\sqrt{s}}{2\pi}\int_{-\infty}^{+\infty} X(\omega)\Phi^*(s\omega)\exp(j\omega t)d\omega$$

$$= \frac{\sqrt{s}}{2\pi}\int_{-\infty}^{+\infty} 2\pi A\delta(\omega-\omega_o)\Phi^*(s\omega)\exp(j\omega t)d\omega$$

$$= A\sqrt{s}\Phi^*(s\omega_o)\exp(j\omega_o t) \qquad (51)$$

Then,

$$|CWT_x(t,s)|^2 = A^2 s\Phi(s\omega_o)\Phi^*(s\omega_o). \qquad (52)$$

To find the scale of maximum correlation, we set the derivative of (52) with respect to s equal to zero:

$$\frac{\partial|CWT_x(t,s)|^2}{\partial s} = 0. \qquad (53)$$

The solution of (53) which provides $s > 0$ is the solution we use. This type of scale to frequency relation provides us, as mentioned before, with an unbiased instantaneous frequency estimator for pure sinusoid without noise.

Acknowledgments

Ervin Sejdić is grateful to Professor Bruno Torrésani from Université de Provence in Marseille, France for his valuable comments regarding the instantaneous frequency estimation using wavelet analysis.

References

[1] B. Tacer and P. Loughlin, "Instantaneous frequency and time-frequency distributions," in *Proc. of IEEE International Conference on Acoustics, Speech, and Signal Processing (ICASSP 1995)*, vol. 2, Detroit, MI, USA, May 09–12, 1995, pp. 1013–1016.

[2] B. Boashash, "Estimating and interpreting the instantaneous frequency of a signal - part 1: Fundamentals," *Proceedings of the IEEE*, vol. 80, no. 4, pp. 520–538, Apr. 1992.

[3] ——, "Estimating and interpreting the instantaneous frequency of a signal - part 2: Algorithms and applications," *Proceedings of the IEEE*, vol. 80, no. 4, pp. 540–568, Apr. 1992.

[4] L. Cohen, *Time-Frequency Analysis*. Englewood Cliffs, N.J: Prentice Hall PTR, 1995.

[5] F. Hlawatsch and G. Boudreaux-Bartels, "Linear and quadratic time-frequency signal representations," *IEEE Signal Processing Magazine*, vol. 9, no. 2, pp. 21–67, Apr. 1992.

[6] P. Rao and F. J. Taylor, "Estimation of instantaneous frequency using the discrete Wigner distribution," *Electronics Letters*, vol. 26, no. 4, pp. 246–248, Feb. 1990.

[7] S. G. Mallat, *A Wavelet Tour of Signal Processing*, 2nd ed. San Diego: Academic Press, 1999.

[8] I. Daubechies, *Ten Lectures on Wavelets*. Philadelphia: Society for Industrial and Applied Mathematics, 1992.

[9] R. Carmona, W.-L. Hwang, and B. Torrésani, *Practical Time-Frequency Analysis: Gabor and Wavelet Transforms with An Implementation in S*. San Diego: Academic Press, 1998.

[10] M. Vetterli and J. Kovačević, *Wavelets and Subband Coding*. Englewood Cliffs, NJ: Prentice Hall, 1995.

[11] M. Unser and A. Aldroubi, "A review of wavelets in biomedical applications," *Proceedings of the IEEE*, vol. 84, no. 4, pp. 626–638, Apr. 1996.

[12] S. Pittner and S. Kamarthi, "Feature extraction from wavelet coefficients for pattern recognition tasks," *IEEE Transactions on Pattern Analysis and Machine Intelligence*, vol. 21, no. 1, pp. 83–88, Jan. 1999.

[13] L. Angrisani, P. Daponte, M. D'Apuzzo, and A. Testa, "A measurement method based on the wavelet transform for power quality analysis," *IEEE Transactions on Power Delivery*, vol. 13, no. 4, pp. 990–998, Oct. 1998.

[14] P. Schroder, "Wavelets in computer graphics," *Proceedings of the IEEE*, vol. 84, no. 4, pp. 615–625, Apr. 1996.

[15] N. Delprat, B. Escudié, P. Guillemain, R. Kronland-Martinet, P. Tchamitchian, and B. Torrésani, "Asymptotic wavelet and Gabor analysis: extraction of instantaneous

frequencies," *IEEE Transactions on Information Theory*, vol. 38, no. 2, pp. 644–664, Mar. 1992.

[16] R. A. Carmona, W. L. Hwang, and B. Torrésani, "Characterization of signals by the ridges of their wavelet transforms," *IEEE Transactions on Signal Processing*, vol. 45, no. 10, pp. 2586–2590, Oct. 1997.

[17] ——, "Multiridge detection and time-frequency reconstruction," *IEEE Transactions on Signal Processing*, vol. 47, no. 2, pp. 480–492, Feb. 1999.

[18] M. I. Todorovska, "Estimation of instantaneous frequency of signals using the continuous wavelet transform," Dept. of Civil Engineering, University of Southern California, Technical Report, 2001.

[19] J. D. Harrop, S. N. Taraskin, and S. R. Elliott, "Instantaneous frequency and amplitude identification using wavelets: Application to glass structure," *Physical Review E*, vol. 66, no. 2, pp. 026 703–1–026 703–9, Aug. 2002.

[20] R. A. Scheper and A. Teolis, "Cramér-Rao bounds for wavelet transform-based instantaneous frequency estimates," *IEEE Transaction on Signal Processing*, vol. 51, no. 6, pp. 1593–1603, Jun. 2003.

[21] S. Meyers, B. Kelly, and J. O'Brien, "An introduction to wavelet analysis in oceanography and meteorology: With application to the dispersion of Yanai waves," *Monthly Weather Review*, vol. 12, no. 10, pp. 2858–2866, Oct. 1993.

[22] C. Torrence and G. P. Compo, "A practical guide to wavelet analysis," *Bulletin of the American Meteorological Society*, vol. 79, no. 1, pp. 61–78, Jan. 1998.

[23] J. D. Harrop, "Structural properties of amorphous materials," Ph.D. dissertation, University of Cambridge, Cambridge, UK, Feb. 2004.

[24] LJ. Stanković and V. Katkovnik, "Algorithm for the instantaneous frequency estimation using time-frequency distributions with adaptive window width," *IEEE Signal Processing Letters*, vol. 5, no. 9, pp. 224–227, Sep. 1998.

[25] V. Katkovnik and LJ. Stanković, "Instantaneous frequency estimation using the Wigner distribution with varying and data-driven window length," *IEEE Transactions on Signal Processing*, vol. 46, no. 9, pp. 2315–2326, Sep. 1998.

[26] V. N. Ivanović, M. Daković, and LJ. Stanković, "Performance of quadratic time-frequency distributions as instantaneous frequency estimators," *IEEE Transactions on Signal Processing*, vol. 51, no. 1, pp. 77–89, Jan. 2003.

[27] LJ. Stanković and V. Katkovnik, "Instantaneous frequency estimation using higher order L-Wigner distribution with data-driven order and window length," *IEEE Transactions on Information Theory*, vol. 46, no. 1, pp. 302–311, Jan. 2000.

[28] LJ. Stanković, V. N. Ivanović, and M. Daković, "Performance of spectrogram as IF estimator," *Electronics Letters*, vol. 37, no. 12, pp. 797–799, Jun. 2001.

[29] V. Ivanović, M. Daković, I. Djurović, and LJ. Stanković, "Instantaneous frequency estimation by using time-frequency distributions," in *Proc. of IEEE International Conference on Acoustics, Speech, and Signal Processing (ICASSP 2001)*, vol. 6, Salt Lake City, UT, USA, May 7–11, 2001, pp. 3521–3524.

[30] Z. M. Hussain and B. Boashash, "Multicomponent IF estimation: a statistical comparison in the quadratic class of time-frequency distributions," in *Proc. of IEEE International Symposium on Circuits and Systems (ISCAS 2001)*, vol. 2, Sydney, NSW, Australia, May 6–9, 2001, pp. 109–112.

[31] M. Daković, V. N. Ivanović, and LJ. Stanković, "On the S-method based instantaneous frequency estimation," in *Proc. of Seventh International Symposium on Signal Processing and Its Applications (ISSPA 2003)*, vol. 1, Paris, France, Jul. 1–4, 2003, pp. 605–608.

[32] LJ. Stanković, I. Djurović, and R.-M. Laković, "Instantaneous frequency estimation by using the Wigner distribution and linear interpolation," *Signal Processing*, vol. 83, no. 3, pp. 483–491, Mar. 2003.